PROCEEDINGS, 24th Annual PNOC-EDC Geothermal Conference
Hotel Inter-Continental, Makati City, Philippines, March 12-13, 2003

EFFECTS OF pH ELEVATION BY NaOH DOSING ON THE CORROSION POTENTIAL OF STEAM CONDENSATES FROM THE UPPER MAHIAO POWER STATION, LEYTE, PHILIPPINES

Ruperto R. Villa, Jr.[1], June Rizza V. Paraon[1], and Keith A. Lichti[2]

[1]PNOC Energy Development Corporation, Merritt Road, Fort Bonifacio, Taguig City, Philippines
[2]Materials Performance Technologies, Industrial Research Limited, Lower Hutt, New Zealand

ABSTRACT

CO_2 rich steam condensate from Upper Mahiao was diverted to the spray tower to elevate the pH to around 6.1 to 7.0 from as low as 4.5. The resulting solution that is aerated is still corrosive to carbon steel construction materials with corrosion rates of 0.4 to 1.0 mm/yr with localized pitting attack. Treating the degassed and aerated condensate with NaOH to adjust its pH to 7.5, gives a drop in the corrosion rate to around 0.3 to 0.5 mm/yr measured using on-line electrical resistance type Corrosometer^{TM} probes and weight loss corrosion coupons in short term tests. The drop in corrosion rate, however, was still above the acceptable corrosion rate set at 0.12 mm/yr and localized pitting was still observed. However, on-line probes suggested a decrease in corrosion rate as a function of time, implying that lower rates would be observed for long-term exposures.

Mineralogy and morphology of corrosion products collected from the carbon steel materials were evaluated using surface analytical techniques such as XRD, EPMA, SEM with EDX, and reflected light microscopy. Magnetite was found in the corrosion products for both the treated and untreated condensate while goethite was observed only when the condensate was treated with NaOH. Iron, sulfur and oxygen were found in all of the samples analyzed by EPMA and SEM, suggesting the presence of an iron sulfur compound,. Potential-pH diagram showed that the stable products are pyrite, troilite and magnetite in this system.

Increase in pH shifted the equilibrium of the solution and dissociation of acid components H_2CO_3 and H_2S into less corrosive species This species change is accompanied by aeration of the fluid in the spray tower and the combined chemistry resulted in the formation of films containing magnetite, goethite and presumably hydrated ferrous sulfate. It is postulated that the formed films have some protective properties but it is recognized that the corrosion rate decrease with pH increase may be a complex function of carbonate and sulfur species as well as oxygen concentration.

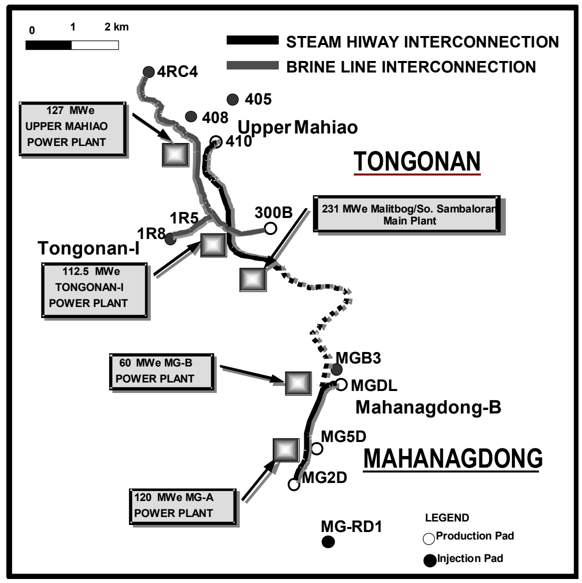

Figure 1. Power stations location, Leyte, Philippines.

1.0 INTRODUCTION

The Upper Mahiao Power Station is part of the Leyte production field in the Philippines (Fig. 1). It has four Geothermal Combined Cycle Units (GCCU) with a total generation capacity of 127 MWe. There is a backpressure steam turbine generator operating at high pressure, which is followed downstream by sets of Ormat Energy Converters (OECs). The OECs operate on an Organic Rankine Cycle using pentane as motive fluid (Salonga et. al., 1998).

The power plant yields a large volume of steam condensate that is corrosive to carbon steels that in this instance are the preferred materials for condensate reinjection pipelines and wells. PNOC EDC will operate a Zero Effluent Disposal Scheme (ZEDS) in Leyte starting January 1, 2003. The ZEDS will be imposed by the Department of Environment and Natural Resources (DENR) and it will require that the condensate that has a maximum flow of 290 kg/s will need to be disposed by injection to the reservoir using the 4RC wells (Fig. 1). It is desired to use existing carbon steel brine reinjection lines to transport the fluid to reinjection wells. Initial experience indicated that a low carbon steel pipeline used to transport this condensate was heavily corroded within three months of commissioning (20 mm in 3 months). Subsequent studies indicated that the corrosion was caused by the presence of high levels of dissolved gases in the condensate (CO_2 and H_2S) which decreased the pH to as low as 4.5 (Salonga et al., 1998). Degassing of the condensate using a spray tower nozzle system was proved useful in elevating the pH from 4.5 to as high as 6.1 to 7.0. However, the condensate was still corrosive to the carbon steel pipeline steels even at this elevated pH (Villa et. al., 2000).

It was proposed to treat the degassed and aerated condensate with NaOH as a means of reducing the corrosion rate. Two NaOH dosing tests were done, one at a pH of 7.5 and one at a pH of 8.0. This paper provides a summary of the initial trials with degassed and pH adjusted condensate. Corrosion rates were determined using ASTM type coupons and electrical resistance Corrosometer™ probes. Analysis results on the corrosion products formed on the carbon steel samples tested at pH 7.5 are presented and initial mechanistic interpretations are given to help in understanding the reasons for the observed corrosion of the pH adjusted, degassed and aerated condensate from the Upper Mahiao Geothermal Power Station.

2.0 METHODOLOGY

2.1 Field Tests

The steam condensate from the Upper Mahiao Power Station was derived from heat exchangers operated at near atmospheric pressure. The majority of the non-condensable gases CO_2 and H_2S were separated off in the power station but the condensing process does give significant dissolved gas. The condensate temperature after degassing was 42 to 43ºC.

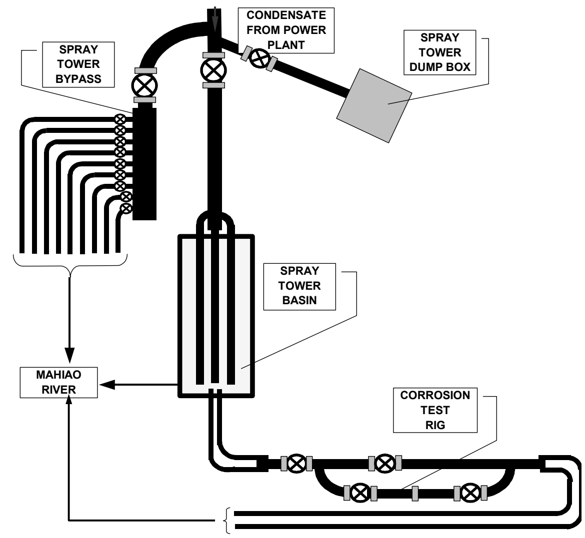

Figure 2. Upper Mahiao spray tower corrosion test-1 monitoring set-up.

Figure 2 shows the degassing system and the location of the corrosion test cell. Three corrosion tests were completed using electrical resistance Corrosometer[TM] probes made from AISI 1010 carbon steel and weight loss coupons of four common construction materials, an ordinary carbon steel (A36), forged steel wellhead material (WHM) and two casing materials (K55 and L80). Figures 3 and 4 show the test arrangements used; triplicate coupons were exposed at each of three locations, the top, side and bottom of the test spool. Figures 5 and 6 show the modified set-up used for the NaOH injection, pH adjustment tests.

Test-1: Condensate After Degassing and Aerating

In this test, the condensates from the spray tower basin were diverted into the corrosion test rig (Fig. 2). The condensate flow rate was 154,080 L/h [42.8 kg/s]. The corrosion coupons were attached to the coupon holder (Fig. 3) and inserted into the test spool and the Corrosometer[TM] probes were inserted into the on-line test spool (Fig. 4) in the top and bottom portions of the spool. Daily pH and Corrosometer[TM] probe corrosion rate

[TM] Corrosometer, Rohrback Cosasco Systems, USA (put this in the footnote)

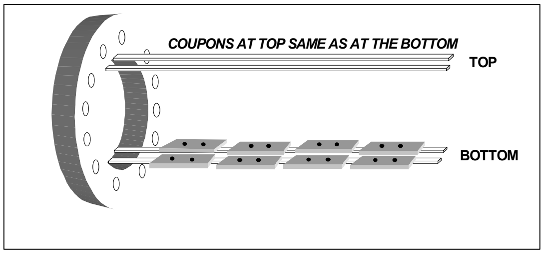

Figure 3. Coupons on coupon holder.

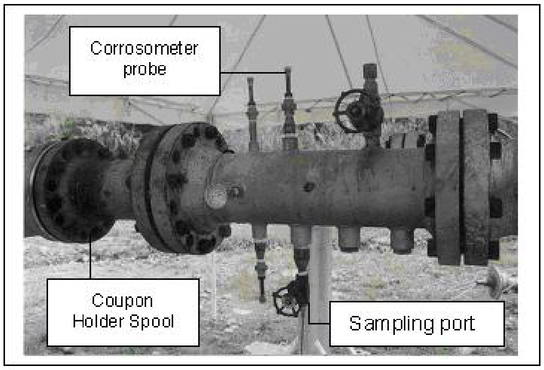

Figure 4. Corrosion test rig with coupon spool and corrosometer probes.

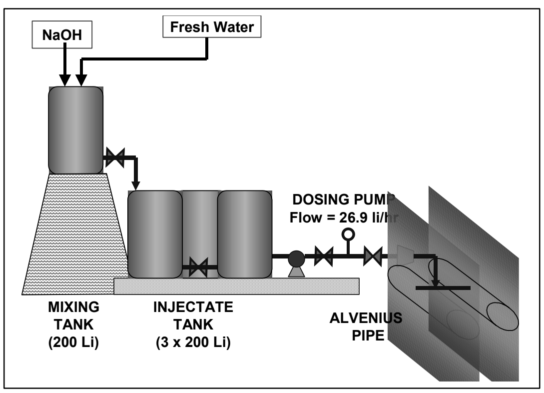

Figure 5. NaOH dosing setup.

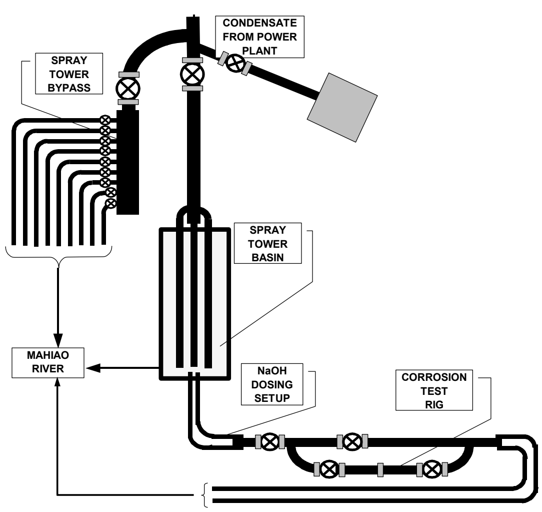

Figure 6. Test-2 and Test-3 Monitoring Setup

measurements were made. Water chemistry sampling was conducted twice a week. The testing started on November 7, 2000 and ended on December 5, 2000. After the testing, the exposed corrosion coupons were cleaned using tri-ammonium citrate with cathodic protection applied and weight loss due to corrosion used to calculate annual corrosion rates by a linear extrapolation. The 5 deepest pits were located and marked under a low power binocular microscope. The depth of localized pitting corrosion observed on the cleaned coupons was quantified using a Lietz DMR optical microscope and a through focus technique and calibrated focus knob on the microscope stage.

Test-2: Increasing the pH of Condensate to 7.5

Using the same initial set-up as in Test-1, a NaOH dosing facility (Fig. 5) was installed upstream of the test rig (Fig. 6). The condensate flow rate was still 154,080 L/h [42.8 kg/s] and NaOH dosing was done at 26.9 L/h using a 7.68% NaOH concentrated solution as injectate. New sets of corrosion coupons and Corrosometer^{TM} probes were used. The coupon exposure was interrupted at the start of the experiment for 25 days, with no condensate flow, while the injection pump was unavailable. Corrosometer^{TM} probes were removed during this time period. A test duration of 30 days was used in the calculations of corrosion rate rather than the 55 days total time, a conservative approach. Daily pH and Corrosometer^{TM} probe readings were taken. Weekly chemistry sampling was conducted. Test-2 dosing was started on January 5, 2001 and ended on February 5, 2001. At the end of the testing, the exposed corrosion coupons were firstly processed by collection of formed and deposited corrosion products for analysis, before they were processed for weight loss and corrosion rate determination as for Test-1.

Test-3: Increasing the pH of Condensate to 8.0

Again, using the same set-up as in Figure 6, a higher pH was obtained by lowering the flowrate of the condensate to 90,000 L/h [25.1 kg/s] by closing one of the pipe lines supplying the corrosion rig with condensate and NaOH dosing was done at 11.9 L/h using 12% NaOH as injectate. One new Corrosometer^{TM} probe (placed in the top port of the test spool) and a new set of corrosion coupons were installed in the setup. Daily pH and Corrosometer^{TM} probe readings were taken and weekly chemistry sampling was conducted. The Test-3 dosing started on November 28, 2001 and ended on December 28, 2001. At the end of the testing, the exposed corrosion coupons were processed for weight loss and corrosion rate determination as for Test-1 and Test-2.

2.2 Corrosion Product Characterization Using Surface Analytical Techniques

The surface structure and composition of the corrosion products formed on the carbon steel materials from the untreated condensate and from the NaOH-dosed condensate at pH~7.5 were examined using the following surface analytical techniques applied to as exposed samples and polished cross sections:

- Binocular and reflected light microscopy,
- X-ray Diffraction (XRD),
- Electron Probe Microanalysis (EPMA),
- Scanning Electron Microscopy with Energy Dispersive X-ray spectrometer (SEM EDX).

Carbon steel samples (A36, forged WHM, K55 and L80) from each of the top, side and bottom sections of the corrosion rig were observed using a binocular microscope. The surface structure of the corrosion products were studied using the Scanning Electron Microscope to observe the appearance and crystallinity of the different mineral phases observed. Energy dispersive X-ray analysis was performed to determine the elemental composition of selected areas of the corrosion products. The elements present in the sample were identified using Energy Dispersive X-Ray Analysis equipment. Polished sections of corrosion products were then prepared for reflected light microscopy. Samples were chosen based on the number of mineral phases present when these were viewed using the binocular microscope and on their location in the corrosion test rig.

X-ray diffraction analysis was performed on parts of the corrosion product to determine the chemical composition of the corrosion products formed on the carbon steel coupons. A Philips PW 1130 high voltage X-ray generator was used together with a Philips PW 1050/25 goniometer, which was fitted with a PW 1752 curved graphite crystal monochromator and PW 1965 proportional detector. To identify the compounds present in the sample, the diffractograms were analyzed using the UPDSM computer software, which matches the spectra obtained from the sample with a spectra database.

The polished samples were analyzed using EPMA to determine the elemental compositions of selected areas of the sample. X-ray detection was done by a PGT Prism 2000 Si (Li) EDS detector with a Be window, interfaced to Moran Scientific pulse-processor/multi-channel amplifier hardware. The identity and weight percent concentration of the elements present in the sample were ascertained using Moran Scientific EDS Quant software. The detection limit for most elements was in the order of 0.3% w/w.

3.0 RESULTS AND DISCUSSION

3.1 On-line Corrosometer^{TM} Probes

Corrosometer results for the three experiments are given in Figures 7 to 9. Figure 10 shows the condensate chemistry for the three tests.

Figure 7 illustrates the trend in on-line corrosion as measured by the Corrosometer^{TM} probes without NaOH dosing (Test-1). This test had a pH range from 6.1 to 7.0 achieved by the degassing process (Fig. 10). The Corrosometer^{TM} probes were previously used and both probes reached end of life in this experiment at about 13 and 9 days for the top and bottom probes respectively. The probes used had an original wall thickness of 0.254 mm. Curve fitting gave rough approximations of corrosion rates at the end of life period and these were extrapolated to 1 year, linear rate of 0.63 mm/y for the top probe and semi parabolic rate equation giving 0.42 mm/year for the bottom probe. The corrosion rates were about 5 times higher than the acceptable corrosion rate of 0.12 mm/yr. The corrosion at this stage was attributed to the limited efficiency of the spray tower to totally remove the dissolved gases in the condensate (Fig. 10). The role played by dissolved oxygen was not known. Additional treatment (i.e. by neutralization with NaOH) was proposed for trial as a means of increasing the pH and lowering the corrosion. There was minimal indication of passive film being developed on the metal element of the probe.

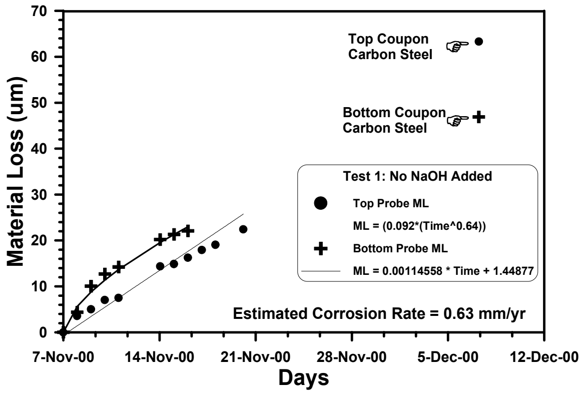

Figure 7. Test-1 Material Loss (ML) vs. Time.

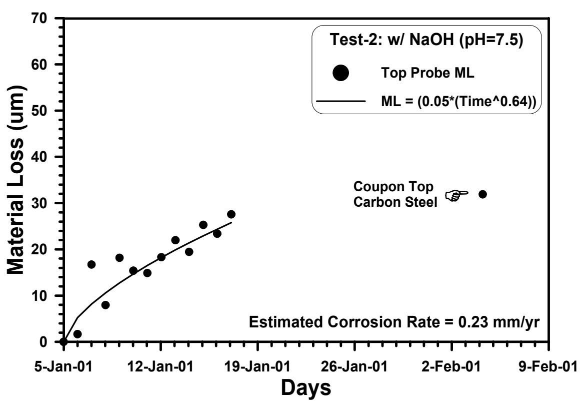

Figure 8. Test-2 Material Loss (ML) vs. Time.

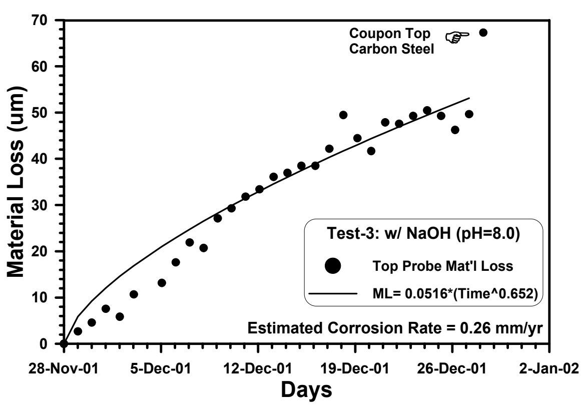

Figure 9. Test-3 Material Loss (ML) vs. Time.

When the 2N NaOH was injected (Test-2) at a rate of 26.9 L/h, the Corrosometer^{TM} probe corrosion rates were noted to drop to 0.23 mm/yr for the top probe using a semi parabolic curve fit (Fig. 8). Again the previously used probe in the top port corroded to perforation in 12 days (the bottom probe failed early in the test and a reliable result was not obtained). The Corrosometer^{TM} probe result with dosing was

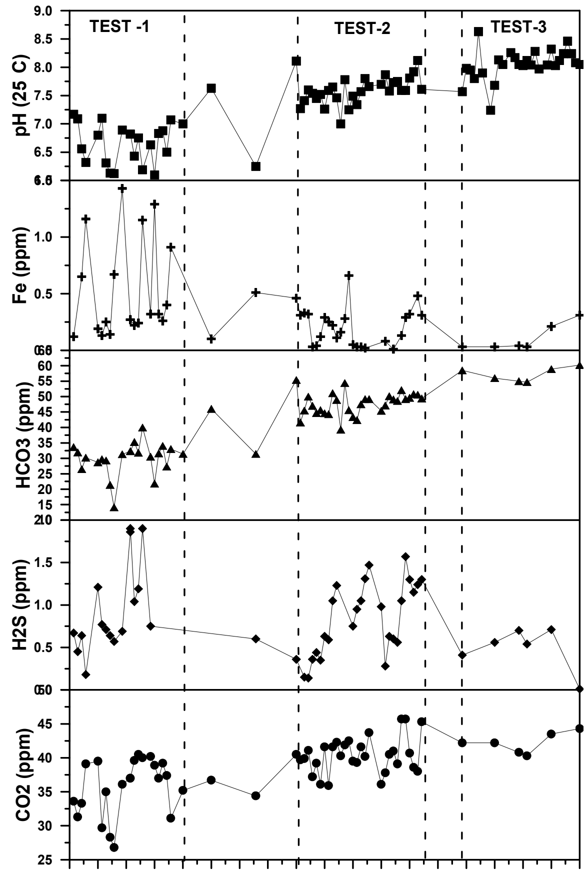

Figure 10 Condensate chemistry during the 3 tests.

more stable compared with those obtained without dosing (compare Fig. 8 with Fig. 7). The deposits formed were partially adherent to the underlying steel.

In the third test with the condensate pH at ~8.0, the corrosion rate from the Corrosometer^{TM} probe used in the top position was 0.28 mm/yr using an extrapolation for a semi parabolic curve fit. This is about the same as observed at pH 7.5 (compare Fig. 9 with Fig. 8). This probe did not perforate in the time of the experiment, i.e. local pitting was decreased.

3.2 Corrosion Coupons

The average surface corrosion rates observed for coupons in the 30 day duration Test-1 were 0.86 mm/yr, 0.66 mm/yr, 0.49 mm/yr and 0.82 mm/yr for L-80 casing, K-55 casing, wellhead material and low carbon steel respectively. The coupons placed at the bottom part of the rig showed the greatest corrosion for each set of materials. The material loss observed on the carbon steel coupons exposed in Test-1 at the

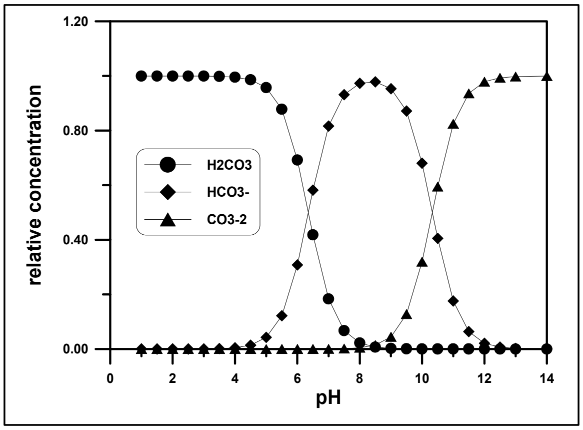

Figure 11. Dissociation of H_2CO_3 as a function of pH (Hargis, 1988).

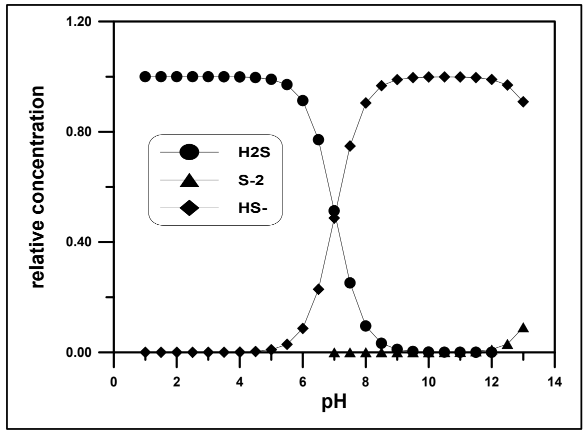

Figure 12. Dissociation of H_2S as a function of pH (Hargis, 1988)

top and bottom locations are shown in Figure 7 for comparison with the Corrosometer™ results. The corrosion products observed were soft, coarse-textured flakes, slightly adherent and easily removed by scraping.

The nominal 30 day Test-2 duration corrosion coupons had calculated average corrosion rates of 0.42 mm/yr, 0.49 mm/yr, 0.49 mm/yr and 0.54 mm/yr for L-80 casing, K-55 casing, wellhead material and carbon steel respectively. The annual coupon corrosion rates were of a similar magnitude or slightly lower compared to those measured by the top Corrosometer™ probe, as illustrated in Figure 8. The corrosion products formed with the treated condensate at pH~7.5 were slightly more adherent compared to those obtained from Test-1.

The calculated corrosion rate results of the corrosion coupons used in the 30 day duration Test-3 were 0.83 mm/yr, 0.72 mm/yr, 0.72 mm/yr and 0.82 mm/yr for L-80 casing, K-55 casing, wellhead material and carbon steel respectively. These results are similar to those obtained without NaOH treatment. But what was significant was the observed corrosion products that deposited on the coupons were again more adherent. The calculation of corrosion rate from the coupon weight loss was by a linear extrapolation and the coupon results are somewhat higher than the Corrosometer™ results predicted from a parabolic curve fit (Fig. 9).

The optical inspection and pit depth measurements revealed a non-planar corroded surface on the pH 6 coupons with surface variations and local pits, on average 0.28 mm (maximum 0.43 mm). A more planar surface attack was observed on the pH 7.5 and pH 8 cleaned coupons with discrete pitting and crevice corrosion evident. At pH 7.5 after the nominal 30 day exposure the average pit depths were only marginally reduced compared to no NaOH being 0.2 mm, however, in one instance, carbon steel on the bottom, the pitting was more than twice the norm at 0.68 mm. This deep pit was anomalous and may have occurred during the period of no flow. The magnitude of the pit depths was less at pH 8 for 30 days, being on average 0.15 mm (maximum 0.26 mm) and relatively uniform for all the materials and locations tested.

3.3 Condensate Chemistry

Presented in Fig. 10 is the trend with time of the different chemical parameters with and without chemical dosing. After the pH was raised by dosing with NaOH, the significant changes observed include a drop in the dissolved Fe level, which suggest that the corrosion rate may have been decreasing or more Fe is being precipitated on internal surfaces. This was coupled with the increase in bicarbonate, HCO_3^- concentration due to the degree of ionization of carbonic acid, H_2CO_3 as a function of pH and the dissolved H_2S gases also dropped at pH~7.5 for the same reason (Figs. 11 and 12).

3.4 Corrosion Products Characterization

The results of the surface analysis undertaken on corrosion products removed from coupons exposed in Test-2 are in agreement with the corrosion rate measurements and point to the presence of iron oxide, iron hydroxide and a sulfur-bearing iron compound on the three carbon steel materials analyzed, carbon steel A36, K55 and L80.

The samples were all magnetic suggesting the presence of a magnetic iron oxide, which in this case was most probably magnetite. Observation of the samples using the binocular microscope indicated the presence of magnetite, which appears as a black, opaque material under the microscope. Another mineral phase, which was prevalent in all of the samples, was a shiny, rust-colored material. This material, based on its appearance was initially thought to be goethite, FeO(OH). Interestingly, the grain sizes of the samples also varied. The corrosion flakes formed from the condensate, which has undergone NaOH treatment generally have coarser size. A brassy-colored yellow phase is also seen in a few samples, which suggested the presence of an iron sulfur compound, possibly a hydrated ferrous sulfate ($FeSO_4.xH_2O$).

Results of the X-ray diffraction analysis are shown in Table 1. They show that the corrosion product common in all of the samples is magnetite (Fe_3O_4). Goethite (FeO(OH)) occurs only in the samples exposed to the condensate treated with NaOH. The goethite is present regardless of whether the corrosion products were formed on the top or bottom of the corrosion rig. Electron microprobe analysis confirmed the presence of Fe, S and O in the samples, however, the form of the iron-sulfur compounds remained elusive.

The surface morphology of the samples is illustrated in Figures 13 and 14. The SEM micrographs revealed that the corrosion products formed on the carbon steel exposed to the condensate treated with NaOH had a more ordered crystalline structure with larger crystals (Fig. 14) while the corrosion products from the untreated condensate show a less well defined crystal structure and appear to have greater porosity as seen by the holes in the product (Fig. 13). Energy dispersive X-ray spectroscopy (EDX) analysis confirmed the presence of the elements Fe, S and O, but again failed to suggest the form of the iron-sulfur compounds present.

Table 1. Samples for X-ray diffraction analysis.

Sample	Location	Condensate Treatment	Compounds Present
L-80	top	Untreated	Fe_3O_4
	bottom		
K-55	top	Untreated	Fe_3O_4
	bottom		
A-36	top	Untreated	Fe_3O_4
	bottom		
L-80	top	with NaOH	Fe_3O_4, FeO(OH)
	bottom		Fe_3O_4, FeO(OH)
K-55	top	with NaOH	Fe_3O_4
	bottom		Fe_3O_4, FeO(OH)
A-36	top	with NaOH	Fe_3O_4, FeO(OH)
	bottom		Fe_3O_4, FeO(OH)

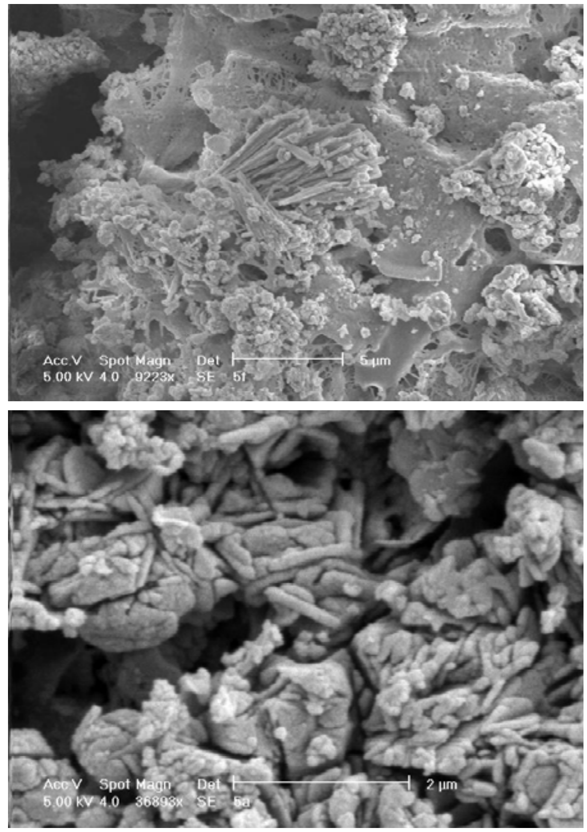

Figure 13. Scanning electron micrographs of corrosion products formed on carbon steel exposed to untreated condensate. The morphology of the sample shows that it has a poorly defined crystalline structure and appears to be porous.

3.5 Chemistry and Corrosion Products

It can be argued that by adding NaOH into the degassed and aerated condensate, the equilibrium conditions for Test-2 and Test-3 were shifted due to the increase in pH. This process forced the acid species carbonic acid (H_2CO_3) to dissociate into its non-acidic

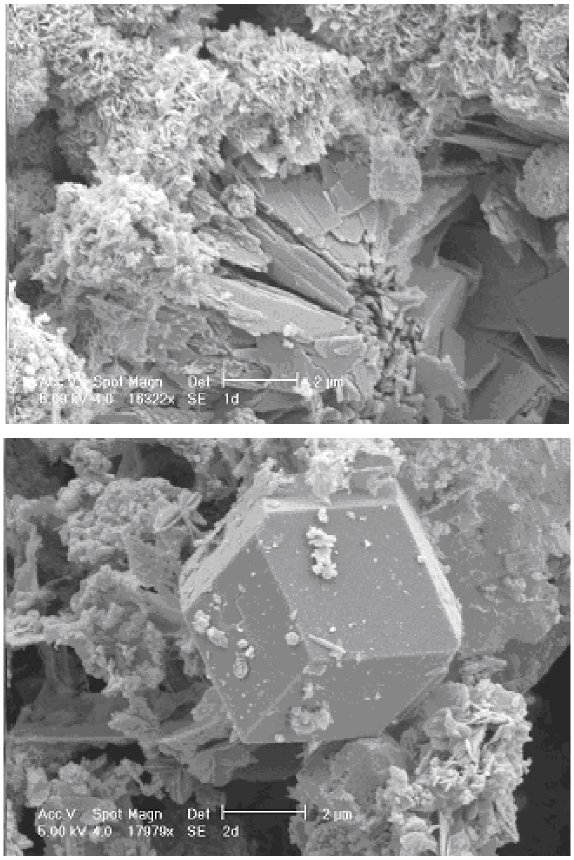

Figure 14. Scanning electron micrographs of corrosion products formed on carbon steel exposed to condensate treated with NaOH. The sample is characterized by a well-defined crystalline structure, of reduced porosity.

component bicarbonate (HCO_3^-) with the dissociated H^+ being neutralized by the added OH^-. The dissociation is demonstrated by the relative concentration of H_2CO_3 as a function of pH in Figure 11. The shift in theoretical equilibrium was confirmed by the observed increase in the concentration of HCO_3^- as shown by the chemistry of the condensate at pH~7.5 (Fig. 10). At this pH level, the dissolved H_2S is less buffered than the CO_2 (compare Fig. 11 with Fig. 12). At pH~8.0, the H_2S in Figure 10 is further reduced. This suggests that more of the H_2S was dissociated into its non-acid specie (HS^-) as the equilibrium of the solution was shifted towards pH~8.0. This is demonstrated in Figure 12. The addition of NaOH appeared to be sufficient to buffer the effect of the dissolved acid gases in the solution and the dissolved Fe concentration dropped suggesting the fluid became less corrosive particularly in Test-3 (Fig. 10).

The increase in pH by NaOH treatment influenced the mineralogy and morphology of the corrosion products. Corrosion products consisting primarily of magnetite formed in the untreated condensate appeared porous and did not have a well-defined crystalline structure as seen by scanning electron microscope (Fig. 13). On the other hand, the corrosion products from the condensate treated with NaOH, again primarily magnetite, but with a definite crystal structure (Fig. 14) and a decrease in the porosity that can potentially be attributed to the formation of a fine grain size FeO(OH) being deposited at the higher pH effectively sealing the pores.

4.0 SUMMARY

The decreasing corrosion rates measured using the on-line probes appear to be a function of increasing pH. The degassed condensate with pH adjusted to 7.5 and 8.0 had similar predicted long term (Corrosometer™) corrosion rates and these were on the order of 0.3 mm/y. This was associated with the formation of more adherent semi protective films of magnetite plus goethite but the presence of oxygen promoted localized corrosion in the higher pH solutions. The influence of pitting on the thin walled Corrosometer™ probes was seen as premature failure of the probes. Notably, the pH 8.0 probe did not perforate.

The corrosion rates measured using coupons show an initial decrease in average corrosion at pH 7.5 and a slightly higher rate when the pH was adjusted to 8.0. Pitting corrosion was most severe on the pH 7.5 coupons possibly due to the lack of flow for a period of time at the start of the experiment. The on-line Corrosometer™ probe results suggest that the linear extrapolation of coupon results is not valid. Rather, the corrosion products formed provide a degree of passivation and lower corrosion rates are predicted.

Chemistry measurements and theoretical consideration suggest that the addition of NaOH resulted in acid species in the solution being dissociated into non-acid species. As more NaOH was added the pH moved towards more alkaline levels, which in effect shifted the equilibrium of the solution to levels sufficient for complete dissociation (Figs. 11 to 12). The lowering of the surface corrosion rate can be attributed to the formation of less corrosive carbonate species but the increase in localized corrosion is attributable to the presence of oxygen.

Degassing the condensates that emanated from the Upper Mahiao power plant GCCU units to increase the pH gives a significant cost savings in NaOH. This process also avoids formation of sulfur as would be predicted if the gas rich solution were pH adjusted by addition of NaOH to the more acid solution. However, use of a spray tower, introduces a limit to the extent of gas removal and introduces dissolved oxygen. The limit in gas removal is due to the relative solubility of the gases with respect to the temperature. The pH adjustment and introduction of oxygen gives an apparent change in the adhesive properties and porosity of the corrosion products and reduces the uniform corrosion rate, but promotes localized corrosion. Increasing the pH from 7.5 to 8.0 gives a reduction in the depth of pitting but additional data are required to confirm the predictions made from the short-term tests and to quantify the long term pitting corrosion rate.

REFERENCES

Gao, W. (1999). Introduction to corrosion and oxidation. Lecture Notes on Materials Performance. Department of Materials Engineering, The University of Auckland.

Hargis, L.G. (1998). Analytical hemistry: Principles and Techniques. Prentice-Hall Inc.

Mortimer, C.E. (1986). Chemistry 6th ed. Wadsworth Publishing Company. California.

Paraon, J.R.V. (2001). Characterization of corrosion products on carbon steel exposed to steam condensates from the Upper Mahiao power station, Leyte, Philippines. *Proceedings, 23rd Annual PNOC-EDC Geothermal Conference, pp. 91-98.*

Salonga, N.D., Villa, Jr., R.R., and Arones, R.G. (1997). Disposal management of steam condensates from a 125 MW direct condensation power plant Upper Mahiao, Leyte, Philippines. *PNOC-EDC Internal Report.*

Salonga, N.D., Villa, Jr., R.R. and Magdadaro, M.C. (1998). Pipeline corrosion in condensate solution containing carbon dioxide and hydrogen sulfide Upper Mahiao Sector, Leyte, Philippines. *PNOC-EDC Internal Report.*

Talens, M.A. and Alcober, E.H. (1999). Corrosion in lowtTemperature fluids with low dissolved gases: the case of condensate pipelines in Malitbog-South Sambaloran sector, Tongonan, Philippines. *PNOC-EDC Internal Report.*

Villa, Jr., R.R. (2001). On-line corrosion test results of the Upper Mahiao spray tower condensates. *PNOC-EDC Internal Report.*

Villa, Jr, R. R., Alcober, E.H. and Paraon, J.R.V. (2000). Corrosion potential and corrosion control of power plant condensates from Leyte geothermal field, Philippines. *PNOC-EDC Internal Report.*

Villa, Jr., R.R, Alcober, E.H., Paraon J.R.V. and Talens, M.A. (2001). Corrosion rates in the different condensate lines of the Leyte geothermal production field, Philippines. *Proceedings, 22nd Annual PNOC-EDC Geothermal Conference, pp. 239-245.*